the Journal of
Molecular
Diagnostics

jmdjournal.org

TECHNICAL ADVANCE

Multiplexed Quantification of Four Neuroblastoma DNA Targets in a Single Droplet Digital PCR Reaction

Check for updates

Constantin Peitz,*[†] Annika Sprüssel,*[†] Rasmus B. Linke,*[†] Kathy Astrahantseff,* Maddalena Grimaldi,*[†] Karin Schmelz,*[‡§] Joern Toedling,* Johannes H. Schulte,*[‡§¶] Matthias Fischer,[‖**] Clemens Messerschmidt,[††‡‡] Dieter Beule,[††] Ulrich Keilholz,[§§] Angelika Eggert,*[‡§¶] Hedwig E. Deubzer,*[†‡§¶] and Marco Lodrini*[†]

From the Department of Pediatric Hematology and Oncology,* Charité−Universitätsmedizin Berlin, Berlin; the Neuroblastoma Research Group,[†] Experimental and Clinical Research Center, and the Core Unit Bioinformatics,[††] Charité−Universitätsmedizin Berlin and the Max Delbrück Center for Molecular Medicine in the Helmholtz Association, Berlin Institute of Health,[¶] Berlin; the German Cancer Consortium, partner site Berlin,[‡] Berlin; the German Cancer Research Center,[§] Heidelberg; the Department of Experimental Pediatric Oncology,[‖] University Children's Hospital of Cologne, Cologne; the Center for Molecular Medicine Cologne,** Cologne; the Department of Computer Science,[‡‡] Humboldt-Universität zu Berlin, Berlin; and the Charité Comprehensive Cancer Center,[§§] Berlin, Germany

The detection and characterization of cell-free DNA (cfDNA) in peripheral blood from neuroblastoma patients may serve as a minimally invasive approach to liquid biopsy. Major challenges in the analysis of cfDNA purified from blood samples are small sample volumes and low cfDNA concentrations. Droplet digital PCR (ddPCR) is a technology suitable for analyzing low levels of cfDNA. Reported here are two quadruplexed ddPCR assay protocols that reliably quantify *MYCN* and *ALK* copy numbers in a single reaction together with the two reference genes, *NAGK* and *AFF3*, and accurately estimate *ALK*^{F1174L} (exon 23 position 3522, C>A) and *ALK*^{R1275Q} (exon 25 position 3824, G>A) mutant allele fractions using cfDNA as input. The separation of positive and negative droplets was optimized for detecting two targets in each ddPCR fluorescence channel by the adjustment of the probe and primer concentrations of each target molecule. The quadruplexed assays were validated using a panel of 10 neuroblastoma cell lines and paired blood plasma and primary neuroblastoma samples from nine patients. Accuracy and sensitivity thresholds in quadruplexed assays corresponded well with those from the respective duplexed assays. Presented are two robust quadruplexed ddPCR protocols applicable in the routine clinical setting and that require only minimal plasma volumes for the assessment of *MYCN* and *ALK* oncogene status. *(J Mol Diagn 2020, 22: 1309−1323; https://doi.org/10.1016/j.jmoldx.2020.07.006)*

Neuroblastoma, a neuroectodermally derived embryonic tumor and the most common extracranial tumor of childhood, accounts for 11% of cancer-related deaths in children world wide, mostly due to systemic and resistant relapses.[1] It is characterized by a heterogeneous tumor biology and, hence, clinical variability ranging from spontaneous regression or localized, stable disease to rapid metastasizing progression with a fatal outcome.[2] The basic helix-loop-helix transcription factor, N-myc proto-oncogene protein (MYCN), regulates the migration, proliferation, and differentiation of the neural crest progenitor cells.[3] *MYCN* amplification occurs in approximately 25% of

primary human neuroblastomas to increase the rate of DNA synthesis, promote cell cycle progression, and suppress differentiation.[4] *MYCN* amplification is a strong predictive biomarker for unfavorable patient survival,[5] and

indirect approaches to target binding partners or downstream effectors of MYCN have yielded encouraging results.[6] Recent data suggest that *MYCN* amplification can exist at the (sub)clonal level, necessitating the use of biosampling procedures and technologies with the capacity for detecting these cell populations.[7,8] Activating mutations in the anaplastic lymphoma kinase gene (*ALK*), occur in approximately 10% of neuroblastomas, the most frequent causing the F1174L and R1275Q substitutes in the receptor tyrosine kinase domain.[9−12] The resulting proteins are auto-hyperphosphorylated and cause uncontrolled proliferation. ALK-driven neuroblastomas, often relapses that may have expanded from a single ALK-mutant clone,[13] are frequently resistant to chemo- and radiotherapy.[9,10,14] Activating *ALK* mutations or amplifications have become the first target in the treatment of neuroblastomas that is directly druggable by small-molecule inhibitors as a personalized medicine approach,[15,16] necessitating continuous molecular monitoring in patients with neuroblastoma for potential (re)emergence of ALK mutant or amplified clones. Clinical testing for *ALK* variants is performed using a broad spectrum of methodologies, including next-generation sequencing, targeted-panel sequencing, and droplet digital (dd)−PCR. Gold standards for *ALK* diagnostics in routine clinical care are expected to evolve within the framework of clinical trials, and are likely to comprise two complementary untargeted and targeted technologies applied, at least initially, in partially overlapping analyses for longitudinal patient monitoring to keep costs affordable.

The invasive nature of surgical biopsies most often prevents their sequential application in monitoring disease. Single biopsies also fail to reflect cancer dynamics, intratumor heterogeneity, and drug sensitivities that most likely change during clonal evolution and under the selective pressure of therapy. Peripheral blood has several components that have been assessed for tumor-derived nucleic acid content.[17−19] Thus, longitudinal patient monitoring using liquid biopsies may represent a promising strategy for patient care, although caution should be exercised in generalizing from the limited data available at this time.

ddPCR is a highly sensitive, recently developed technology for quantifying specific regions.[20,21] The ddPCR reaction reagents are partitioned into 20,000 droplets before reactions are allowed to proceed to the end plateau in individual droplets; then droplets are classified as positive or negative from their fluorescence signal intensity. Duplex ddPCR protocols for detecting *MYCN* and *ALK* copy number status in cell-free (cf)-DNA purified from patient plasma samples have been previously established.[22] Combaret et al[23] presented ddPCR protocols for detecting ALK^{F1174L} and ALK^{R1275Q} hotspot mutations, each together with the respective wild-type sequence in duplex reactions. Here, the blood sample volumes sequentially required from infants and young children, the patients most often affected by neuroblastoma, were minimized by the extension of multiplexing for the generation of robust quadruplexed ddPCR protocols.

Materials and Methods

Patient Samples

Paired blood plasma and fresh-frozen primary tumor samples were collected from patients treated at Charité−Universitätsmedizin Berlin (Berlin, Germany) or provided by the German Neuroblastoma Biobank (Cologne, Germany). All patients were registered with the German NB2004 trial or the NB 2016 Registry, and informed patient/parent consent was obtained before trial participation. Peripheral blood was centrifuged at $1900 \times g$ for 7 minutes at Charité and at $1000 \times g$ for 10 minutes at the German Neuroblastoma Biobank to separate plasma. After centrifugation at $3250 \times g$ for 10 minutes to remove cell debris, plasma was stored at $-80°C$. The *ALK* copy number in tumor samples was determined as a routine diagnostic method using fluorescence *in situ* hybridization.

Cell Culture

The BE(2)-C cell line was obtained from the European Collection of Authenticated Cell Cultures (Salisbury, UK), and Kelly and SH-SY5Y cell lines, from the Deutsche Sammlung von Mikroorganismen und Zellkulturen (Braunschweig, Germany). The CLB-GA [established in the Centre Léon BERARD (CLB), Lyon, France[24]] as well as the IMR-5, LAN-5, and LAN-6 cell lines were kindly gifted by Johannes H. Schulte (Charité−Universitätsmedizin Berlin); the NB-1 cell line, by Ina Oehme (German Cancer Research Center, Heidelberg, Germany); and the SH-EP and SK-N-AS cell lines, by Larissa Savelyeva (German Cancer Research Center). Cell lines were authenticated by high-throughput single-nucleotide polymorphism−based assays.[25] Genomic cell line characteristics are summarized in Supplemental Table S1.[9−12,26−46] The BE(2)-C, CLB-GA, SH-SY5Y, and SK-N-AS cell lines were maintained in Dulbecco's modified Eagle's medium (Lonza, Cologne, Germany) supplemented with 10% fetal calf serum and 1% nonessential amino acids. The LAN-6 cell line was cultured in Dulbecco's modified Eagle's medium supplemented with 20% fetal calf serum. The IMR-5, Kelly, LAN-5, NB-1, and SH-EP cell lines were cultured in RPMI 1640 medium (Lonza) supplemented with 10% fetal calf serum and 1% nonessential amino acids. All cell lines were maintained at 37°C and 5% CO_2, and continuous culture was avoided to maintain low passage numbers and to reduce the risk for long-term culture-induced genomic alterations. Cells for experiments were grown in short-term culture from low-passage stock aliquots maintained in liquid nitrogen. All cell lines were regularly monitored for infection with *Acholeplasma laidlawii*, *Mycoplasma* spp, and squirrel monkey retrovirus using high-throughput, multiplexed testing.[47]

Genomic DNA and cfDNA Preparation

Genomic DNA (gDNA) was extracted from tumor tissues and cell lines using the Puregene Core Kit A or the QIAamp DNA Mini Kit (both from Qiagen, Hilden, Germany) according to the manufacturer's instructions. gDNA from cell lines was fragmented by sonication before ddPCR. Tumor DNA could not be sonicated because of the small sample volumes (20 µL), and fragmentation was achieved by adding 5 U of HindIII restriction enzyme (New England BioLabs, Frankfurt am Main, Germany) to each ddPCR reaction. Thawed plasma samples were centrifuged at $2000 \times g$ for 5 minutes to clear debris, then supernatants were centrifuged at $20,000 \times g$ for 5 minutes. cfDNA was purified from a minimum of 200 µL of stored plasma samples using the QIAamp Circulating Nucleic Acid Kit (Qiagen), then concentrated to 50 µL using the DNA Clean & Concentrator-5 kit (Zymo Research, Freiburg, Germany), both according to the manufacturers' directions. cfDNA did not require fragmentation prior to ddPCR. Extracted DNA samples were quantified on a Qubit 2.0 fluorometer (Life Technologies, Darmstadt, Germany). The Cell-Free DNA ScreenTape assay and the TapeStation 4200 system (both from Agilent Technologies, Santa Clara, CA) were used for DNA quality-control samples according to the manufacturer's instructions.

Droplet Digital PCR

The QX200 ddPCR System (Bio-Rad Laboratories, Munich, Germany) was used for analyzing the copy number statuses of *MYCN* (2p24.3), *ALK* (2p23.2 to 2p23.1), *NAGK* (2p13.3), and *AFF3* (2q11.2), and for detecting *ALK* F1174L (exon 23 position 3522, C>A) and R1275Q (exon 25 position 3824, G>A) hotspot mutations with their corresponding wild-type sequences. TaqMan ddPCR reaction mixtures contained the $2\times$ ddPCR Supermix for Probes (no deoxyuridine triphosphate) (Bio-Rad Laboratories) and optimized primer and probe concentrations (Tables 1 and 2)[23,48] in a total volume of 20 µL. Primer3 software version 0.4.0 was used for primer and probe design.[49] To confirm the specificity of the probes used for the detection of ALK^{F1174L} (3522, C>A) and ALK^{R1275Q} (3824, G>A), four double-stranded synthetic *ALK* templates with the following sequences were generated (Metabion, Planegg, Germany): ALK^{F1174L} (3522, C>A, TTC>TTA), 5′-GCCCAGACTCAGCTCAGTTAATTTTGGTTACATCCCTCTCTGCTCTGCAGCAAATTAAACCACCAGAACATTGTTCGCTGCATTGGGG-3′; ALK^{F1174L} (3522, C>G, TTC>TTG), 5′-GCCCAGACTCAGCTCAGTTAATTTTGGTTACATCCCTCTCTGCTCTGCAGCAAATTGAACCACCAGAACATTGTTCGCTGCATTGGGG-3′; ALK^{R1275Q} (3824, G>A, CGA>CAA), 5′-GTCCAGGCCCTGGAAGAGTGGCCAAGATTGGAGACTTCGGGATGGCCCAAGACATCTACAGGTGAGTAAAGACTGCCTCACCCC-3′; and ALK^{R1275L} (3824, G>T, CGA>CTA), 5′-GTCCAGGCCCTGGAAGAGTGGCCAAGATTGGAGACTTCGGGATGGCCCTAGACATCTACAGGTGAGTAAAGACTGCCTCACCCC-3′. The probe established for the detection of ALK^{F1174L} (3522,

C>A) reliably detected this but not the ALK^{F1174L} (3522, C>G) mutation. The probe established for the detection of ALK^{R1275Q} (3824, G>A) detected only this and not the ALK^{R1275L} (3824, G>T) mutation (Supplemental Figure S1), together confirming the specificity of the probes selected.

Reaction mixtures were loaded into droplet generator cartridges together with 70 µL Droplet Generation Oil (both from Bio-Rad). Droplets were generated in the QX200 droplet generator, and manually transferred into a 96-well PCR plate (Eppendorf, Hamburg, Germany) according to the manufacturer's recommendations. The PCR plate was heat-sealed with the PX1 Plate Sealer (Bio-Rad), and PCR reactions were performed on a T100 thermocycler (Bio-Rad), with the following programs for copy number variations: denaturation at 95°C for 10 minutes, 40 cycles of 30 seconds at 94°C and 1 minute at 58°C, and final denaturation for 10 minutes at 98°C; and for *ALK* hotspot mutation analysis: denaturation at 95°C for 10 minutes, 40 cycles of 30 seconds at 94°C and 1 minute at 62.5°C, and final denaturation for 10 minutes at 98°C. Droplet reaction end points were assessed in the QX200 ddPCR Droplet Reader. Target gene copy numbers and mutant allele fractions (MAFs) were analyzed using QuantaSoft Analysis software version 1.7.4.0917 and QuantaSoft Analysis Pro software version 1.0.596 (Bio-Rad). All multiplex ddPCR assays contained appropriate nontemplate, positive and negative controls in each run to allow the software programs to generate specific thresholds.

The QuantaSoft Analysis software used for duplex ddPCR assays determined the copy number by calculating the ratio of target molecule concentration, A (copies/µL), to the reference molecule concentration, B (copies/µL), multiplied by the number of reference species copies, N_B, in the human genome (Copy number $= A/B \cdot N_B$). The QuantaSoft Analysis Pro software used triplex and quadruplex ddPCR assays for determining the copy number by calculating the ratio of the target molecule concentration, A, to the geometric mean of the reference molecule concentrations, B (copies/µL) and C (copies/µL), multiplied by the number of reference species copies, N_B, (Copy number $= A/[\text{geomean}(B,C)] \cdot N_B$). *MYCN* and *ALK* amplifications were designated as the detection of ≥ 8.01 copies, with gain (defined as the detection of 2.74 to 8.00 copies) and normal diploid status (defined as the detection of 1.50 to 2.73 copies).[22] The false-positive rate and lower limit of detection for point mutation analyses were calculated with Bio-Rad lookup tables in line with the model by Armbruster and Pry.[50] In principle, false-positive rate calculation was based on two parameters. The number of false-positive droplets and the minimally required concentration of mutant target molecules (copies/µL) for each point-mutation protocol were defined by analysis of gDNA from cell lines with the wild-type sequence of the respective mutation. A sample was scored as positive if both the number of droplets detecting the mutation and the concentration of mutant target molecules (copies/µL) were above the set thresholds.

Table 1 Sequences and Concentrations of Primers and Probes Used in Multiplexed ddPCR Protocols to Assess *ALK* and *MYCN* Copy Number Status

Primer/Probe	Sequence	Concentration, nmol/L		
		Duplex ddPCR	Triplex ddPCR	Quadruplex ddPCR
AFF3-for	5′-CACCTAGCATGTGTGGCATT-3′	900	900	900
AFF3-rev	5′-GCAGATCCAGGTCGTTGAAG-3′	900	900	900
AFF3-probe	5′-HEX-AACAACTCTTTCTGTCCCCCT-BHQ1-3′	250	125	125
ALK-for	5′-CTTGTCCTCTGACTCTTCTCG-3′	900	900	300
ALK-rev	5′-CAAGACTCCACGAATGAGC-3′	900	900	300
ALK-probe	5′-FAM-TCACAGCTCCGAATGTCCTG-BHQ1-3′	250	250	360
MYCN-for*	5′-GTGCTCTCCAATTCTCGCCT-3′	900	900	450
MYCN-rev*	5′-GATGGCCTAGAGGAGGGCT-3′	900	900	450
MYCN-probe*	5′-FAM-CACTAAAGTTCCTTCCACCCTCTCCT-BHQ1-3′	250	250	125
NAGK-for*	5′-TGGGCAGACACATCGTAGCA-3′	900	900	900
NAGK-rev*	5′-CACCTTCACTCCCACCTCAAC-3′	900	900	900
NAGK-probe*	5′-HEX-TGTTGCCCGAGATTGACCCGGT-BHQ1-3′	250	350	350

*Adapted from Gotoh et al.[48]

FAM, 6-carboxyfluorescein; HEX, hexachloro-fluorescein.

The lower limit of detection was determined for each assay by measuring a 1:10 to 1:100,000 mix of DNA derived from cell lines with (SH-EP, CLB-GA) or without (SK-N-AS) the respective mutations. Thresholds were separately calculated for 0.5, 2, 10, 20, 80, and 130 ng of input DNA in duplex and quadruplex formats.

WES of Matched cfDNA and Tumor Samples

Whole-exome sequencing (WES) libraries were prepared with the Agilent SureSelect XT kit version 6 (Agilent Technologies) according to the manufacturer's protocol. For sequencing, four to five libraries were pooled in the flow cell to be sequenced (100-bp, paired-end) in one lane on the HiSeq 4000 sequencer (Illumina, San Diego, CA), with a median of 84 million fragments per sample. Standard quality control was performed using FastQC version 0.11.9 (*http://bioinformatics.babraham.ac.uk/projects/fastqc*, last accessed February 20, 2020). Reads were aligned to the GRCh37 reference sequence using BWA-MEM software version 0.7.15.[51] Separate read groups were assigned for all reads from one lane, and duplicates were masked using Samblaster software version 0.1.24.[52] *MYCN* and *ALK* copy numbers were estimated using CNVkit[53] version 0.9.6 on each WES library without a normal control, as described by the manufacturer. Digital copy numbers in tumor samples were calculated as $(2 \cdot 2^{\log_2 FC} - 2 + 2 \cdot p)/p$. The log$_2$ fold-change, Log_2FC, of a given gene was estimated to a diploid baseline by CNVkit, and p was the tumor cell content. Tumor samples had at least 70% tumor cells. Copy numbers derived from cfDNA analysis were calculated by setting the tumor cell content to 1.

WES of Neuroblastoma Cell Lines

DNA was extracted from the human neuroblastoma cell lines BE(2)-C, Kelly, LAN-6, and SH-SY5Y using the NucleoSpin Tissue kit (Macherey-Nagel, Düren, Germany) according to

Table 2 Sequences and Concentrations of Primers and Probes Used in Multiplexed ddPCR Protocols to Detect the Neuroblastoma-Specific *ALK*^{F1174L} and *ALK*^{R1275Q} Hotspot Mutations

Primer/Probe	Sequence*	Concentration, nmol/L	
		Duplex ddPCR	Quadruplex ddPCR
ALK^{1174}-for	5′-GCCCAGACTCAGCTCAGT-3′	900	900
ALK^{1174}-rev	5′-CCCCAATGCAGCGAACAAT-3′	900	900
ALK^{F1174L} probe, FAM	5′-FAM-TCTCTGCTCTGCAGCAAATTAAACC-BHQ1-3′	250	350
ALK^{1174} probe, FAM	5′-FAM-TCTCTGCTCTGCAGCAAATTCAACC-BHQ1-3′	—	50
ALK^{1174} probe, HEX	5′-HEX-TCTCTGCTCTGCAGCAAATTCAACC-BHQ1-3′	250	—
ALK^{1275}-for	5′-GTCCAGGCCCTGGAAGAG-3′	900	600
ALK^{1275}-rev	5′-GGGGTGAGGCAGTCTTTACTC-3′	900	600
ALK^{R1275Q} probe, FAM	5′-FAM-TTCGGGATGGCCCAAGACAT-BHQ1-3′	250	—
ALK^{R1275Q} probe, HEX	5′-HEX-TTCGGGATGGCCCAAGACAT-BHQ1-3′	—	400
ALK^{1275} probe, HEX	5′-HEX-TTCGGGATGGCCCGAGACAT-BHQ1-3′	250	150

*Adapted from Combaret et al.[23]

FAM, 6-carboxyfluorescein; HEX, hexachloro-fluorescein.

the manufacturer's instructions. Libraries for WES were prepared using the SureSelect Human All Exon kit version 7 (Agilent) and the TruSeq Exome kit (Illumina). Libraries were sequenced on HiSeq 4000 and NovaSeq 6000 sequencers (Illumina). Read sequences and base quality scores were demultiplexed and stored in FASTQ format using bcl2fastq software version 2.20 (Illumina). Adapter remnants and low-quality read ends were trimmed off using custom scripts. The quality of the sequence reads was assessed using FastQC software. Reads were aligned to the human genome, assembly GRCh38, using BWA-MEM software,[51] and duplicate read alignments were removed using Samblaster.[52] Copy number variations were determined using CNVkit.[53] Single-nucleotide variants were identified using Strelka2 software version 2.9.10.[54] Potential germline variants were filtered out by excluding all single-nucleotide variants that had also been observed in at least 1% of samples in cohorts of healthy individuals, namely the 1000 Genomes Project[55] and the National Heart, Lung, and Blood Institute's Grand Opportunity Exome Sequencing Project[56] cohorts.

Statistical Analysis

Correlation analyses were performed using GraphPad Prism software version 6.00 (GraphPad Software, San Diego, CA). P values ≤ 0.05 were considered significant.

Results

Developing Quadruplexing to Absolutely Quantify *MYCN* and *ALK* Copy Numbers in a Single ddPCR Assay

Duplex ddPCR assay conditions were previously reported to assess *MYCN* and *ALK* copy numbers in gDNA and cfDNA using *N*-acetylglucosamine kinase gene (*NAGK*) as a reference gene.[22] To save sample volume, which is substantially restricted in infancy and early childhood, a quadruplex ddPCR assay was established for reliable measurement of both gene copy numbers in a single reaction together with two reference genes to increase robustness for normalization. Assay conditions for a triplex reaction were first established, in which *MYCN* or *ALK* was measured in parallel in channel 1 while *NAGK* and a second reference gene, *AFF3*, which is frequently used as a control for fluorescence *in situ* hybridization directed against *MYCN*,[57] were both detected in channel 2. For accurate discrimination between fluorescence amplitudes of negative, single-positive, and double-positive droplet clusters for *AFF3* and *NAGK* in channel 2, a uniplex reaction was performed using fragmented DNA from the SK-N-AS neuroblastoma cell line as a template, in which *AFF3* and *NAGK* probe concentration series ranging from 100 to 400 nmol/L together with a fixed primer concentration of 900 nmol/L for both genes were tested. Optimal separation of *AFF3*-positive and *NAGK*-positive droplet clusters and identical fluorescence amplitude of *AFF3*-negative and *NAGK*-negative droplet clusters as the desired result were used for selecting probe concentrations of

125 nmol/L (*AFF3*) and 350 nmol/L (*NAGK*) for further testing in triplex reactions with these settings (Supplemental Figure S2). Using fragmented DNA from SK-N-AS cells as a template and the previously established primer and probe concentrations for *ALK* and *MYCN* for duplex reactions (Table 1),[22] triplex reactions (*ALK/AFF3/NAGK*, *MYCN/AFF3/NAGK*) were performed and an accurate separation of negative and single-, double-, and triple-positive droplet clusters with *ALK* or *MYCN* in channel 1 and both *AFF3* and *NAGK* in channel 2 were observed (Figure 1).

Probe and primer concentrations for the simultaneous detection of *ALK* and *MYCN* in channel 1 were next established using fragmented SK-N-AS gDNA as a template. Probes for *ALK* and *MYCN* were each tested in the range of 100 to 400 nmol/L in combination with the standard primer concentration (900 nmol/L) for duplex and triplex assays (Table 1) in a uniplex assay. The *ALK* probe concentration of 400 nmol/L and two *MYCN* probe concentrations (125 and 250 nmol/L) were further tested in *MYCN/AFF3* and *ALK/NAGK* duplex reactions (Supplemental Figure S3A). Finalizing conditions were used for absolutely quantifying *MYCN* copy number, and the two probe concentrations were combined, with primer concentrations varying between 225 and 900 nmol/L. Positive and negative droplet clusters were optimally separated using probe and primer concentrations of 125 and 450 nmol/L, respectively, as: i) the bandwidths of both clusters were comparatively smallest, ii) the distance between both clusters was comparatively largest, and iii) the fluorescence amplitudes of *MYCN*-negative and *ALK*-negative droplet clusters were almost identical (Supplemental Figure S3B). The assay conditions were then optimized to absolutely quantify *ALK* copy numbers. The probe range of 350 to 400 nmol/L was tested with 300 or 900 nmol/L primer in the *MYCN/AFF3* and *ALK/NAGK* duplex reactions. While *ALK*-positive and *ALK*-negative droplet clusters were clearly separable with each of the probe/primer combinations tested, 300 nmol/L primer with probe concentrations between 360 and 380 nmol/L was most suited for simultaneous *ALK* and *MYCN* detection in channel 1 (Supplemental Figure S4A). All three *ALK*-specific probe concentrations produced separation of negative and single-, double-, triple-, and quadruple-positive clusters in the *ALK/MYCN/AFF3/NAGK* quadruplex reaction, but with varying degrees of droplet rain between the *ALK* and *MYCN* double-positive cluster. The *ALK* single-positive cluster in channel 1 was smallest with 360 nmol/L *ALK* probe, prompting its selection as the optimized concentration (Supplemental Figure S4, B–D). QuantaSoft Analysis Pro software accurately distinguished a total of 16 different droplet clusters including negative and single-, double-, triple- and quadruple-positive droplets from the two-dimensional plot (Figure 2A and Table 1). Findings from channels 1 and 2 were confirmed in one-dimensional plots (Figure 2, B and C) and histograms (Figure 2, D and E).

The accuracy and sensitivity of the quadruplex ddPCR reaction was compared to those of the triplex and previously published duplex reactions using fragmented SK-N-AS
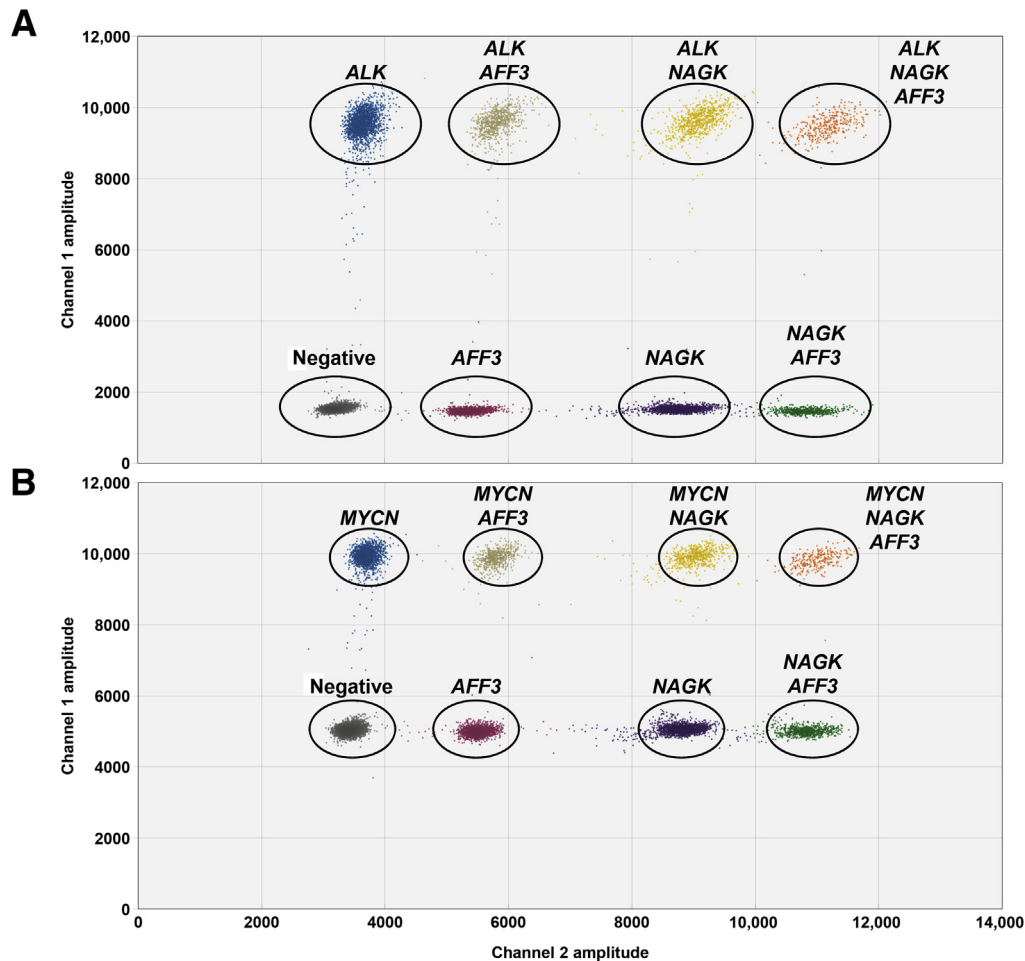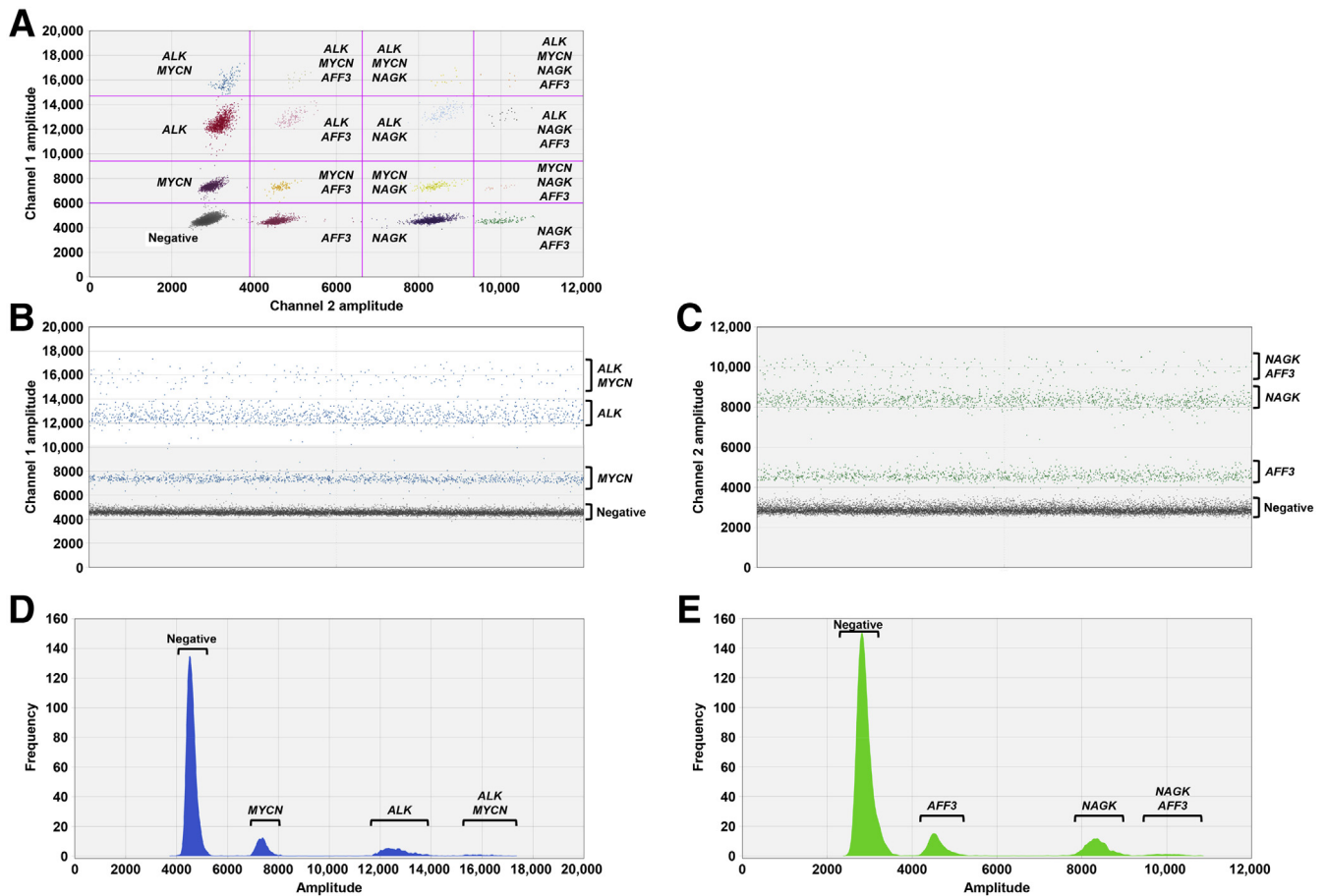
Figure 2   Representative plots and histograms of quadruplex ddPCR assay assessing *ALK* and *MYCN* copy number status. Genomic DNA was extracted from SK-N-AS cells and fragmented by sonication before ddPCR reactions using a total of 10 ng as input material. **A:** Representative two-dimensional plot of droplet fluorescence in the quadruplex reaction. *MYCN* and *ALK* droplets were plotted in channel 1 (6-carboxyfluorescein; FAM) against *AFF3* and *NAGK* droplets in channel 2 (hexachloro-fluorescein; HEX). **Lines** indicate thresholds for negative as well as single-, double-, triple-, and quadruple-positive droplet clusters. **B** and **C:** One-dimensional plots of droplet fluorescence in channel 1 for *MYCN* and *ALK* (**B**) and in channel 2 for *AFF3* and *NAGK* (**C**). Plots document optimal separation of negative, single-positive, and double-positive droplets. **Blue dots** (channel 1) and **green dots** (channel 2) indicate positive droplets; **gray dots** indicate negative droplets. **D** and **E:** One-dimensional fluorescence amplitude histograms indicate the droplet frequency at specific fluorescence amplitudes in channel 1 (**D**, *MYCN* and *ALK*) and in channel 2 (**E**, *AFF3* and *NAGK*). Again, droplet frequencies for negative, single-positive, and double-positive clusters were clearly distinguishable.

cell line were, with 4.32 and 4.27 in the quadruplex and triplex assays, slightly higher than the 3.0 measured in the duplex assay (Figure 3B), most likely again reflecting the more robust normalization in the quadruplex and triplex assay designs. Normal *ALK* diploid status was detected in the LAN-5, IMR-5, and SK-N-AS cell lines (Figure 3B). Copy numbers ranged from 1.99 ± 0.13 to 2.10 ± 0.05 using the quadruplex protocol, which corresponded well with those determined using triplex (1.93 ± 0.24 to 2.13 ± 0.15) and duplex (1.85 ± 0.37 to 2.00 ± 0.25) protocols. For comparison, WES data were generated for the BE(2)-C, Kelly, SH-SY5Y, and LAN-6 cell lines and copy number variations were determined on the p-arm of chromosome 2. This analysis showed a strong focal amplification of the *MYCN* gene locus in the BE(2)-C and Kelly cells (Supplemental Figure S6). Further, the Kelly, SH-SY5Y, and LAN-6 cells showed widespread, albeit weaker, copy number gains, up to four copies in total, in the first 50

megabases of chromosome 2 that include the *ALK* gene locus (Supplemental Figure S6), thus validating the ddPCR results. Interestingly, the WES data showed a loss of heterozygosity in the *AFF3* gene in the Kelly cell line, which explains the different *MYCN* and *ALK* copy number results obtained in those ddPCR assays that included *AFF3* as a second reference gene in the calculation. The data demonstrate robust *MYCN* and *ALK* copy number quantification that clearly distinguishes between amplification, gain, and diploid allele status by the quadruplex ddPCR assay.

Quadruplex ddPCR Can Quantify *MYCN* and *ALK* Copy Numbers from Blood Plasma or Neuroblastoma Samples from Patients

Quadruplex ddPCR-based *MYCN* and *ALK* copy numbers were next assessed in blood plasma samples paired with gDNA from the corresponding primary neuroblastoma from three
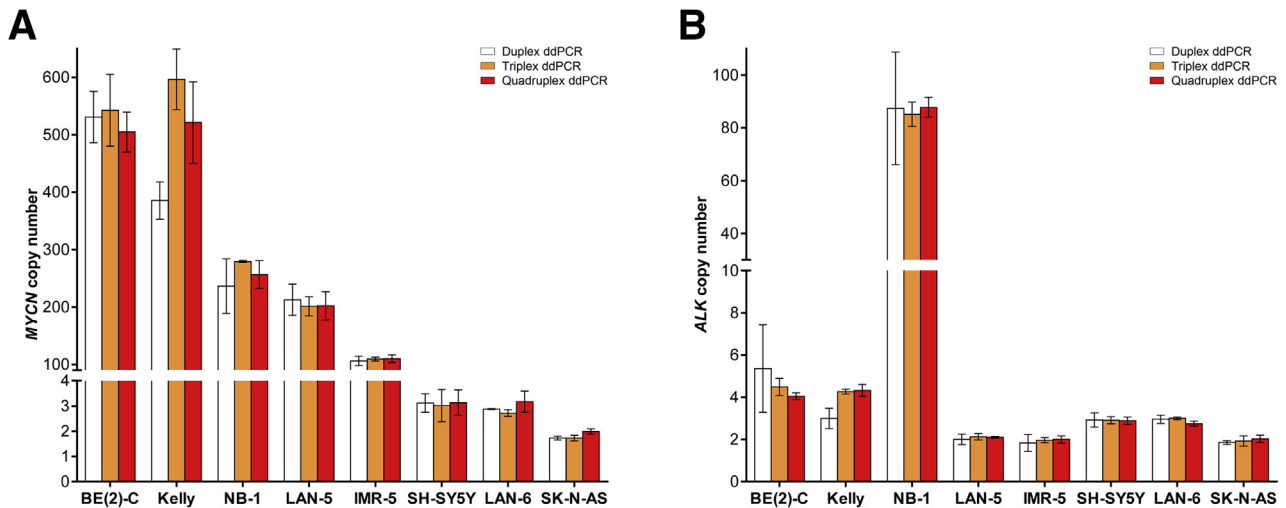
Figure 3 Comparison of absolute *MYCN* and *ALK* copy numbers determined by multiplexed ddPCR assays in neuroblastoma cell lines. **A** and **B**: Genomic DNA was extracted and fragmented by sonication before ddPCR reactions to quantify *MYCN* (**A**) and *ALK* (**B**) copy numbers. A total of 2 ng of DNA was used as input material. Data are expressed as means ± SD. $n \geq 3$.

patients. Results were compared with copy numbers determined by duplex and triplex ddPCR and re-analyzed from WES data, which were deposited in the European Genome-Phenome Archive (accession number EGAS00001004275; https://www.ebi.ac.uk/ega/studies, last accessed March 2, 2020). Quadruplex ddPCR of tumor DNA revealed high-level *MYCN* amplifications in samples from Patients 1 and 2, which were confirmed by duplex and triplex ddPCR reactions and re-analysis of WES tumor data (Table 3). All multiplexed ddPCR assays detected the *MYCN* amplification using cfDNA in plasma from Patients 1 and 2, although the copy numbers estimated were consistently lower than those from direct assessment of tumor DNA (Table 3). Findings were confirmed through re-analysis of WES data from these cfDNA samples (Table 3). The lower copy numbers detected in circulating cfDNA may have stemmed from a dilution effect caused by handling-induced damage to white blood cells in the samples (these blood samples were previously collected for a different purpose) from tumor heterogeneity or cfDNA derived from nontumor cells. Therefore, the DNA quality was evaluated in plasma samples from Patients 1 and 2 using the TapeStation 4200 System. The cfDNA content amounted to 69.8% and 81.1% in these samples, thus pointing either to tumor heterogeneity or the presence of cfDNA derived from nontumor cells (Table 3). Diploid *MYCN* allele status was detected by quadruplex ddPCR using either tumor or cfDNA from Patient 3, and was confirmed by all other assays (Table 3). Quadruplex ddPCR detected an *ALK* gain using either tumor or cfDNA from Patient 1 and diploid *ALK* allele status in Patients 2 and 3 using either DNA source (Table 3). Although the *ALK* gain could not be clearly identified in the WES data, all other results were confirmed in all other assays (Table 3). *ALK* fluorescent *in situ* hybridization was performed on interphase nuclei of a tumor section from Patient 1 and detected three *ALK* copies (Supplemental Figure S7), thus confirming the ddPCR data and a false-negative result in the WES data. The data

consistently demonstrate that absolute *MYCN* and *ALK* copy numbers can be quantified from DNA derived from either tumor or plasma samples from patients, and that quadruplexed ddPCR using two diploid reference genes for normalization is a feasible and sensitive alternative for reducing sample volumes.

Developing Quadruplex ddPCR—Based Detection of ALK^{F1174L} and ALK^{R1275Q} Hotspot Mutations

The *ALK* hotspot mutations at F1174 (C>A conversion at nucleotide 3522 in exon 23) and R1275 (G>A conversion at nucleotide 3824 in exon 25) occurring in neuroblastomas can be detected by duplex ddPCR.[23] It was hypothesized that simultaneous detection of both *ALK* hotspot mutations in a quadruplex ddPCR reaction is technically feasible. As template providing both hotspot mutations and the wild-type *ALK* sequences to develop the quadruplex assay, DNA was extracted from the SH-EP neuroblastoma cell line (harboring a heterozygous ALK^{F1174L} mutation) and mixed 1:1 with DNA extracted from the CLB-GA neuroblastoma cell line (harboring a heterozygous ALK^{R1275Q} mutation). Uniplex and duplex assays determined that 900 and 600 nmol/L primers with 350 and 400 nmol/L probes concentrations were optimal for detecting ALK^{F1174L} and ALK^{R1275Q} target molecules, respectively, in channel 1 (Table 2). Both mutation sites in the wild-type sequence were targeted (ALK^{1174} and ALK^{1275}) to detect wild-type *ALK*, with both clearly detected in channel 2 using 900 and 600 nmol/L primers and 50 and 150 nmol/L probes, respectively (Table 2). Combining ALK^{F1174L} and ALK^{R1275Q} detection in channel 1 with ALK^{1174} and ALK^{1275} detection in channel 2 in a quadruplex reaction allowed no clear identification of individual droplet clusters (data not shown), prompting the application of the concept of an inverted ddPCR protocol described by Alcaide et al.[58]

Table 3 Comparatively Determined *MYCN* and *ALK* Copy Numbers in Patient Samples

Patient	Disease stage	Sample	Tumor cell content, %	cfDNA content, %	*MYCN* copy number				*ALK* copy number			
					Quadruplex ddPCR*	Triplex ddPCR*	Duplex ddPCR*	WES[†]	Quadruplex ddPCR*	Triplex ddPCR*	Duplex ddPCR*	WES[†]
1	M	gDNA	75	—	290.6	239.2	233.9	239.7	3.24	2.80	2.89	2.30
		cfDNA	—	69.8	43.5	48.7	48.9	58.3	3.00	2.89	3.35	2.13
2	M	gDNA	70	—	140.1	135.0	141.4	142.6	2.07	1.97	2.17	1.81
		cfDNA	—	81.1	32.3	36.1	35.1	37.9	1.96	2.40	2.26	1.88
3	M	gDNA	90	—	1.86	1.82	1.64	1.92	2.05	2.17	1.78	1.92
		cfDNA	—	n.a.	2.23	2.68	2.15	1.91	1.70	2.41	2.38	1.91

*DNA input for ddPCR reactions ranged from 1 to 2 ng.

[†]DNA input for WES ranged from 8 to 110 ng.

cfDNA, cell-free DNA; gDNA, genomic DNA; n.a., not analyzed; WES, whole-exome sequencing.

The hexachloro-fluorescein fluorophore on the ALK^{1174} probe was replaced by a 6-carboxyfluorescein fluorophore, and the 6-carboxyfluorescein fluorophore on the ALK^{R1275Q} probe was replaced by a hexachloro-fluorescein fluorophore for the simultaneous detection of ALK^{F1174L} and ALK^{1174} in channel 1 and ALK^{R1275Q} and ALK^{1275} in channel 2. This approach produced accurate separation of negative, single-positive, and double-positive droplet clusters including ALK^{F1174L}/ALK^{1275}, ALK^{1174}/ALK^{1275}, $ALK^{F1174L}/ALK^{R1275Q}$, and ALK^{1174}/ALK^{R1275Q} (Figure 4A). In line with data from previous reports on other inverted ddPCR approaches,[57] some double-double positive clusters (ALK^{F1174L}/ALK^{1174} in channel 1 and ALK^{R1275Q}/ALK^{1275} in channel 2) as well as triple-positive and quadruple-positive droplets were not clearly separable from other droplet clusters (Figure 4A). Findings from channels 1 and 2 were confirmed in one-dimensional plots (Figure 4, B and C) and histograms (Figure 4, D and E). The data demonstrate that an inverted quadruplex ddPCR approach can be used for analyzing the neuroblastoma-specific ALK^{F1174L} and ALK^{R1275Q} hotspot mutations in a single reaction.

The dynamic range of the $ALK^{F1174L}/ALK^{R1275Q}$ quadruplex ddPCR detection was assessed using serially diluted DNA template (0.5 to 130 ng) from the SK-N-AS, SH-EP, or CLB-GA cell line. The detected concentrations of target molecules (ALK^{F1174L}, ALK^{R1275Q}, ALK^{1174}, and ALK^{1275}) were significantly correlated with the theoretically assigned concentrations (Pearson correlation coefficients ranged from 0.9942 to 0.9981) and strongly resembled the concentrations detected in duplex reactions (ALK^{F1174L}/ALK^{1174} and ALK^{R1275Q}/ALK^{1275}), with Pearson correlation coefficients ranging from 0.9871 to 0.9981 (Supplemental Figure S8). The data demonstrate that quadruplex ALK^{F1174L} and ALK^{R1275Q} hotspot mutation detection remains linear within the range of 0.5 to 130 ng of input DNA.

Sensitivity thresholds for *ALK* hotspot mutation detection in quadruplex reactions were also defined and compared to sensitivity in duplex detection. DNA from cell lines harboring either *ALK* hotspot mutation was mixed 1:10 to 1:100,000 with DNA from cell lines with homozygous wild-type *ALK*. Mutant allele fractions (MAFs) were designated as 0% in cells with wild-type *ALK*. A neuroblastoma cell was categorized as harboring an ALK^{F1174L} mutation using the following thresholds: ≥4 positive droplets and at least 0.31 copies/μL for up to 10 ng of input DNA and ≥5 positive droplets and at least 0.57 copies/μL for higher input DNA amounts. These thresholds were very similar to those defined for the duplex reaction (≥4 positive droplets, at least 0.33 copies/μL). The thresholds for categorizing a neuroblastoma cell as harboring an ALK^{R1275Q} mutation varied according to input DNA amounts in both assays (quadruplex reaction, ≥5 to ≥15 positive droplets, 0.42 to 1.34 copies/μL; duplex reaction, ≥4 to ≥17 positive droplets, 0.32 to 1.31 copies/μL). Together, the sensitivity thresholds for the simultaneous detection of both neuroblastoma-specific *ALK* hotspot mutations in quadruplex ddPCR were similar to those for the respective duplex ddPCR reactions.

Quadruplex ddPCR Correctly Assesses ALK^{F1174L} and ALK^{R1275Q} MAFs in Cell Lines

The quadruplex ddPCR assay for *ALK* hotspot mutations was tested in a panel of six neuroblastoma cell lines harboring the ALK^{F1174L} mutation (SH-EP, Kelly[12,34]), the ALK^{R1275Q} mutation (CLB-GA, LAN-5[10,11]), or wild-type *ALK* [SK-N-AS, BE(2)-C[12]]. The ALK^{F1174L} mutation was correctly detected in SH-EP and Kelly cells, and MAFs determined using quadruplex ddPCR corresponded well those determined by duplex ddPCR (Table 4). Both quadruplex and duplex ddPCR correctly detected MAFs indicating that only one allele harbored the mutation. Wild-type *ALK* in both alleles was correctly detected in CLB-GA, LAN-5, SK-N-AS, and BE(2)-C cells using the ALK^{1174} target in quadruplex ddPCR (Table 4). The monoallelic ALK^{R1275Q} mutation was similarly detected in CLB-GA and LAN-5 cells, with strongly corresponding MAFs detected by quadruplex and duplex ddPCR assays (Table 4). The single wild-type *ALK* allele in SH-EP and Kelly cells and the biallelic wild-type *ALK* status in SK-N-AS and BE(2)-C cells were correctly detected using the ALK^{1275} target in
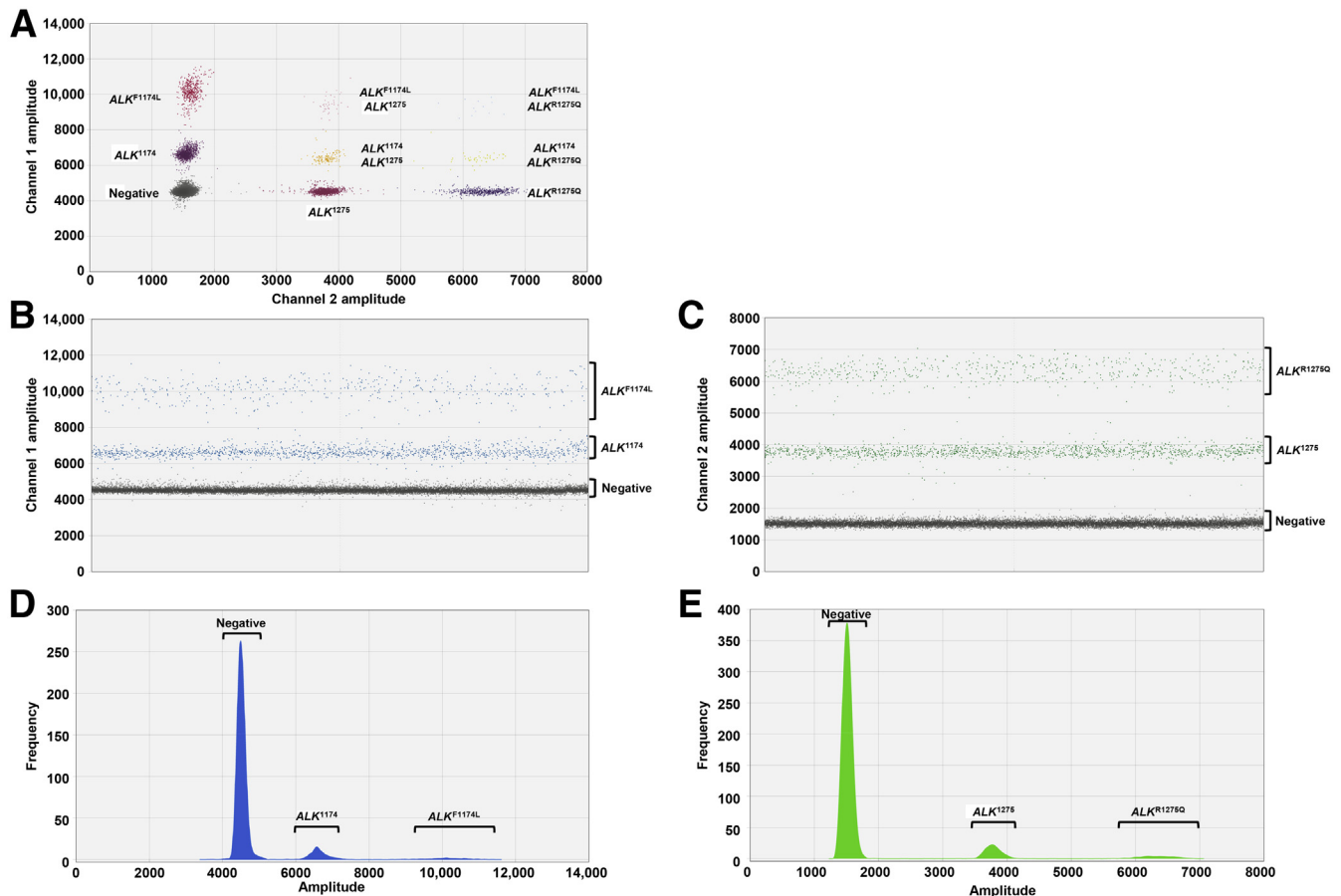
Figure 4 Quadruplex ddPCR assay for the detection of the neuroblastoma-specific hotspot mutations ALK^{F1174L} and ALK^{R1275Q}. For assay design, DNA was extracted from SH-EP (ALK^{F1174L}) and CLB-GA (ALK^{R1275Q}) cells, fragmented by sonication and mixed 1:1 before ddPCR reactions to generate a DNA mixture comprising both mutations. A total of 20 ng of this DNA mixture was used as input material. **A:** Representative two-dimensional plot of droplet fluorescence. ALK^{F1174L} and ALK^{1174} droplets were plotted in channel 1 (6-carboxyfluorescein; FAM) against ALK^{R1275Q} and ALK^{1275} droplets in channel 2 (hexachloro-fluorescein; HEX). Shown are negative, single-positive, and double-positive clusters. **B** and **C:** One-dimensional plots of droplet fluorescence for ALK^{F1174L} and ALK^{1174} in channel 1 (**B**) and for ALK^{R1275Q} and ALK^{1275} in channel 2 (**C**). Plots documented optimal separation of negative and single-positive droplets. **Blue dots** (channel 1) and **green dots** (channel 2) indicate positive droplets; **gray dots** indicate negative droplets. **D** and **E:** One-dimensional fluorescence amplitude histograms indicate the droplet frequency at specific fluorescence amplitudes in channel 1 (**D**, ALK^{F1174L} and ALK^{1174}) and in channel 2 (**E**, ALK^{R1275Q} and ALK^{1275}). Droplet frequencies are clearly distinguishable.

quadruplex ddPCR (Table 4). These findings suggest that quadruplex ddPCR performs well as an assay-validating step in the detection of wild-type *ALK* and *ALK* hotspot mutations in neuroblastoma cell lines.

Quadruplex ddPCR Detects ALK^{F1174L} and ALK^{R1275Q} MAFs in Blood Plasma and Neuroblastoma Samples from Patients

After quadruplex ddPCR was validated in the detection of neuroblastoma-specific *ALK* hotspot mutations in cell lines, the assay was applied to paired blood plasma and tumor samples from six patients with neuroblastoma to compare its accuracy and sensitivity to those of the established duplex ddPCR reactions[23] using both standard tumor biopsies and liquid biopsies suited to longitudinal patient monitoring. The quadruplex ddPCR correctly detected an ALK^{F1174L} mutation in tumor and plasma samples from Patients 4 and 5, with MAFs indicating that a varying proportion of tumor cells harbored the mutation on one allele (although 14% higher in quadruplex detection in cfDNA from Patient 4) (Table 5). No ALK^{F1174L} mutation was detected in matched tumor-derived DNA/cfDNA samples from Patients 6 through 9 by either assay (Table 5). The quadruplex ddPCR assay correctly demonstrated an ALK^{R1275Q} mutation in tumor-derived DNA and plasma-derived cfDNA from Patients 6 to 8, and the MAFs obtained by the two assays very closely resembled each other in all cases except one, which was a 10% higher MAF measured in tumor-derived DNA from Patient 8 by quadruplex ddPCR (Table 5). No ALK^{R1275Q} mutation was detected in matched tumor/blood plasma samples from Patients 4, 5, or 9 by either assay (Table 5). The higher MAFs in cfDNA from Patient 4 and tumor-derived DNA from Patient 8, as determined by quad-ruplex ddPCR compared to duplex ddPCR, prompted the

Table 4   Comparison of Multiplexed ddPCR Assays for Detecting ALK^{F1174L} and ALK^{R1275Q} Mutant Allele Fractions in Neuroblastoma Cell Lines

Cell line*	ALK^{F1174L} (3522, C>A)[†]		ALK^{R1275Q} (3824, G>A)[†]	
	Quadruplex ddPCR	Duplex ddPCR	Quadruplex ddPCR	Duplex ddPCR
SH-EP	45.82 ± 0.87	48.64 ± 0.31	0	0
Kelly	31.58 ± 0.69	31.20 ± 0.52	0	0
CLB-GA	0	0	53.77 ± 0.52	53.04 ± 0.64
LAN-5	0	0	53.55 ± 1.95	51.45 ± 0.82
SK-N-AS	0	0	0	0
BE(2)-C	0	0	0	0

*DNA input, 10 ng.
[†]Mutant allele fraction is shown in mean percentage ± SD for $n \geq 3$ replicates; mutant allele fraction of 0% indicates wild-type *ALK*.

testing of the influence of input quantity on MAF measurement, as the two respective samples contained higher DNA amounts than all other samples analyzed. Fragmented DNA was serially diluted from an ALK^{F1174L} mutant cell line (SH-EP) and an ALK^{R1275Q} mutant cell line (CLB-GA) in H_2O to obtain 0.5, 2, 10, 20, 80, and 130 ng of DNA. ALK^{F1174L} MAF assessment based on 0.5 to 20 ng of total input DNA resulted in similar findings in quadruplex and duplex reactions. Using DNA input amounts of 80 and 130 ng resulted in comparatively higher MAF results in the quadruplex reaction (Supplemental Figure S9A). Similar findings were obtained on analysis of the ALK^{R1275Q} MAF with varying DNA input amounts. Using 0.5 to 20 ng of DNA input, MAF results were similar in the quadruplex and duplex reactions, but were higher in the quadruplex reaction with total input DNA amounts of 80 and 130 ng (Supplemental Figure S9B). This observation was likely due to the underestimation of an increasing amount of wild-type and mutant double-positive droplets in higher DNA input samples in

Table 5   Comparatively Determined ALK^{F1174L} and ALK^{R1275Q} Mutant Allele Fractions in Paired Blood Plasma and Neuroblastoma Samples from Patients

Patient	Sample*	ALK^{F1174L} (3522, C>A)[†]		ALK^{R1275Q} (3824, G>A)[†]	
		Quadruplex ddPCR	Duplex ddPCR	Quadruplex ddPCR	Duplex ddPCR
4	gDNA	48.17	48.36	0	0
	cfDNA	59.29	45.40	0	0
5	gDNA	11.07	12.95	0	0
	cfDNA	36.27	35.20	0	0
6	gDNA	0	0	47.92	48.19
	cfDNA	0	0	32.91	28.90
7	gDNA	0	0	43.48	43.65
	cfDNA	0	0	21.99	22.10
8	gDNA	0	0	87.29	77.96
	cfDNA	0	0	71.90	68.00
9	gDNA	0	0	0	0
	cfDNA	0	0	0	0

*Cell-free DNA input material ranged between 6.9 and 72.6 ng, and gDNA input material ranged between 6.9 and 98.5 ng.
[†]Mutant allele fraction of 0% indicates wild-type *ALK*.
cfDNA, cell-free DNA; gDNA, genomic DNA.

inverted ddPCR protocols because the fluorescence signals of double-positive droplets had an amplitude similar to that of single mutant-positive droplets and might have been obscured in this droplet cluster.[58] Taken together, the data demonstrate that the quadruplex ddPCR protocol accurately distinguishes between ALK^{F1174L}, ALK^{R1275Q}, and wild-type *ALK* in plasma-derived cfDNA and tumor DNA.

Discussion

One of the challenges in infants and children with a body weight of <10 kg is to sequentially obtain sufficient blood volumes for molecular analyses without considerably lowering hemoglobin levels and, ultimately, necessitating an iatrogenically induced blood transfusion. Volumes for blood sampling are therefore ethically restricted to 1 mL in infants and a maximum of 3 mL in children. Experiences with blood samples from neuroblastoma patients indicate that, on average, 10 to 130 ng of cfDNA diluted in 50 μL of elution buffer is available after purification for further analysis. Previously published duplex ddPCR protocols assessing *MYCN* and *ALK* copy numbers using *NAGK* as a single reference gene each require 5 μL of cfDNA extract.[22] ddPCR is a rapid, highly sensitive, less expensive, and more accessible tool for many laboratories compared to next-generation sequencing approaches. It enables targeted analyses of known copy number variations and mutations, while next-generation sequencing enables an unbiased approach, but requires a longer time to obtain, process, and analyze data, with a need for bioinformatics expertise.[59,60] Increasing evidence suggests that the characterization of the cfDNA in plasma from neuroblastoma patients with targeted and untargeted approaches such as ddPCR, real-time quantitative PCR, shallow WES, OncoScan arrays (Affymetrix, Santa Clara, CA), or WES contributes to the understanding of molecular risk factors as well as spatial and temporal heterogeneity in neuroblastoma.[18,19,23,48,61–66]

The technical feasibility of multiplexing DNA targets by ddPCR beyond single and duplex reactions has been exemplarily shown by the quantification of recurrent somatic mutations in diffuse large B-cell and follicular lymphoma tissue sections[58] and scoring programmed cell death protein

ligand 1 in non—small cell lung cancer biopsies.[67] To optimize the amplitude of a droplet cluster in higher-order multiplexing assays, i) probe concentrations, ii) primer concentrations, and iii) annealing temperature in the PCR cycler program can be adapted.[68] After optimization of the first two parameters, simultaneous copy number assessment of two of the major oncogenic drivers in neuroblastoma, *MYCN* and *ALK*, was shown to be technically feasible using *NAGK* and *AFF3* as two normal diploid reference genes. Quality assessment of linearity and lower limit of detection showed highly comparable results between the respective duplex and triplex reactions, saving precious sample volume. While the quadruplexed ddPCR protocol was shown to be a highly sensitive and robust analytical tool for exact assessment of copy number status, it maintains a targeted analysis by nature, which is limited to the analysis of a short range of DNA base pairs, often of <100 nucleotides. This was reflected by a higher *ALK* amplification status in the NB-1 cell line and by the misdetection of a partial *ALK* amplification in the IMR-5 cell line due to the use of primer pairs different from those used for previously reported data.[22] Another example of the targeted nature of the ddPCR technology was the observation that only the WES technology but none of the *ALK* ddPCR assays discriminated between a specific *ALK* gain and copy number gains within the first 50 megabases of chromosome 2p, including the *ALK* gene, in the neuroblastoma cell lines investigated. The WES data reported in the present study are in line with those from previous studies, summarized in Supplemental Table S1. The well-known intrinsic ddPCR assay limitation justifies the combination of this targeted analysis applicable in routine clinical testing at sequential time points for monitoring disease status and the emergence of new potentially druggable targets such as *ALK* or activating Ras—mitogen-activated protein kinase pathway mutations in combination with unbiased next-generation sequencing approaches at a defined time point, such as initial or relapse diagnosis. Other molecular characteristics used in neuroblastoma risk stratification, including DNA ploidy and segmental copy number variations, are not detected with the targeted *MYCN/ALK* quadruplexing ddPCR approach. The ddPCR technology could nonetheless affect clinical decision making by considerably shortening the time needed for switching to a potentially promising alternative targeted therapy, and may, therefore, have considerable potential with regard to its translation into daily clinical practice in the near future. Although the number of studies reporting ddPCR applications in oncology has rapidly increased over recent years, additional prospective studies in larger patient cohorts are needed for further validation.

To increase the robustness of the ddPCR assay in the assessment of *MYCN* and *ALK* copy number status, a second normal diploid reference gene on the 2q arm (*AFF3* at 2q11.2) was included. The incorporation of a second reference gene enables the internal control between both reference genes to detect the unlikely but non-excludable event of a potential copy number variation in a

well-established reference gene in individual patient samples. For example, the approximately 30% higher *MYCN* and *ALK* copy numbers detected by triplex and quadruplex reactions in Kelly cells were attributable to a loss of heterozygosity in *AFF3*. *ALK* copy number assessment in cfDNA purified from plasma samples will enable monitoring in patients with neuroblastoma for the targetable *ALK* amplification in the future. This is important because the treatment of *ALK*-amplified neuroblastoma cell lines with ALK inhibitor was shown to potently suppress ALK downstream signaling and to trigger an apoptotic response *in vitro*.[28,69] *ALK* amplification is emerging as a potential biomarker associated with response to targeted inhibition in neuroblastoma models.[15,16]

The quadruplexed protocol detecting the *ALK* hotspot mutations *ALK*[F1174L] (3522, C>A) and *ALK*[R1275Q] (3824, G>A) is based on the previously reported inverted ddPCR approach,[58] and allows the successful detection and quantification of either or both mutations in a simultaneous reaction in samples with low DNA input. Detection and quantification are possible by changes in the labeled probes and therefore measurement of *ALK*[F1174L] (3522, C>A), together with the respective *ALK*[wild-type] sequence in channel 1, and *ALK*[R1275Q] (3824, G>A) with this corresponding *ALK*[wild-type] sequence in channel 2. In this setting, the respective mutant and wild-type sequences are amplified with the same primer pair, and the reactions compete against each other for the existing resources in the droplet, diminishing the fluorescence signal from double-positive clusters. This well-known phenomenon from duplex reactions[68] leads to a shift of the double-positive clusters in one channel to the upper single-positive clusters. Although the occurrence of double-positive droplets is comparatively low in samples with low DNA input, it increases in high-DNA input samples, causing MAF overestimation for the respective mutation in the calculation. Although the mutant and wild-type sequences are detected in separate channels in duplex reactions and can, thereby, clearly be distinguished from each other, the natural limitation of the inverted ddPCR approach used here necessitates that DNA input be restricted to maximally 20 ng, making it also well-suited for analyzing cfDNA. Here, two novel quadruplexed ddPCR protocols enabled, with high analytical sensitivity and low cost, the assessment of copy number variations and hotspot mutations crucial for monitoring and treating children with neuroblastoma in routine clinical settings.

Research Center High Throughput Sequencing Unit for providing sequencing services; and Johannes H. Schulte, Ina Oehme, and Larissa Savelyeva for sharing CLB-GA, IMR-5, LAN-5, and LAN-6; NB-1; and SH-EP and SK-N-AS cell lines, respectively.

Supplemental Data

Supplemental material for this article can be found at https://doi.org/10.1016/j.jmoldx.2020.07.006.

References

1. Schulte JH, Eggert A: Neuroblastoma. Crit Rev Oncog 2015, 20:245−270
2. Brodeur GM: Neuroblastoma: biological insights into a clinical enigma. Nat Rev Cancer 2003, 3:203−216
3. Grimmer MR, Weiss WA: Childhood tumors of the nervous system as disorders of normal development. Curr Opin Pediatr 2006, 18:634−638
4. Schwab M, Alitalo K, Klempnauer KH, Varmus HE, Bishop JM, Gilbert F, Brodeur G, Goldstein M, Trent J: Amplified DNA with limited homology to myc cellular oncogene is shared by human neuroblastoma cell lines and a neuroblastoma tumour. Nature 1983, 305:245−248
5. Brodeur GM, Seeger RC, Schwab M, Varmus HE, Bishop JM: Amplification of N-myc in untreated human neuroblastomas correlates with advanced disease stage. Science 1984, 224:1121−1124
6. Huang M, Weiss WA: Neuroblastoma and MYCN. Cold Spring Harb Perspect Med 2013, 3:a014415
7. Marrano P, Irwin MS, Thorner PS: Heterogeneity of MYCN amplification in neuroblastoma at diagnosis, treatment, relapse, and metastasis. Genes Chromosomes Cancer 2017, 56:28−41
8. Berbegall AP, Bogen D, Potschger U, Beiske K, Bown N, Combaret V, Defferrari R, Jeison M, Mazzocco K, Varesio L, Vicha A, Ash S, Castel V, Coze C, Ladenstein R, Owens C, Papadakis V, Ruud E, Amann G, Sementa AR, Navarro S, Ambros PF, Noguera R, Ambros IM: Heterogeneous MYCN amplification in neuroblastoma: a SIOP Europe Neuroblastoma Study. Br J Cancer 2018, 118:1502−1512
9. Mosse YP, Laudenslager M, Longo L, Cole KA, Wood A, Attiyeh EF, Laquaglia MJ, Sennett R, Lynch JE, Perri P, Laureys G, Speleman F, Kim C, Hou C, Hakonarson H, Torkamani A, Schork NJ, Brodeur GM, Tonini GP, Rappaport E, Devoto M, Maris JM: Identification of ALK as a major familial neuroblastoma predisposition gene. Nature 2008, 455:930−935
10. Janoueix-Lerosey I, Lequin D, Brugieres L, Ribeiro A, de Pontual L, Combaret V, Raynal V, Puisieux A, Schleiermacher G, Pierron G, Valteau-Couanet D, Frebourg T, Michon J, Lyonnet S, Amiel J, Delattre O: Somatic and germline activating mutations of the ALK kinase receptor in neuroblastoma. Nature 2008, 455:967−970
11. Chen Y, Takita J, Choi YL, Kato M, Ohira M, Sanada M, Wang L, Soda M, Kikuchi A, Igarashi T, Nakagawara A, Hayashi Y, Mano H, Ogawa S: Oncogenic mutations of ALK kinase in neuroblastoma. Nature 2008, 455:971−974
12. George RE, Sanda T, Hanna M, Frohling S, Luther W 2nd, Zhang J, Ahn Y, Zhou W, London WB, McGrady P, Xue L, Zozulya S, Gregor VE, Webb TR, Gray NS, Gilliland DG, Diller L, Greulich H, Morris SW, Meyerson M, Look AT: Activating mutations in ALK provide a therapeutic target in neuroblastoma. Nature 2008, 455:975−978
13. Schleiermacher G, Javanmardi N, Bernard V, Leroy Q, Cappo J, Rio Frio T, Pierron G, Lapouble E, Combaret V, Speleman F, de Wilde B, Djos A, Ora I, Hedborg F, Trager C, Holmqvist BM, Abrahamsson J, Peuchmaur M, Michon J, Janoueix-Lerosey I, Kogner P, Delattre O, Martinsson T: Emergence of new ALK mutations at relapse of neuroblastoma. J Clin Oncol 2014, 32:2727−2734
14. Maris JM: Recent advances in neuroblastoma. N Engl J Med 2010, 362:2202−2211
15. Mosse YP, Lim MS, Voss SD, Wilner K, Ruffner K, Laliberte J, Rolland D, Balis FM, Maris JM, Weigel BJ, Ingle AM, Ahern C, Adamson PC, Blaney SM: Safety and activity of crizotinib for paediatric patients with refractory solid tumours or anaplastic large-cell lymphoma: a Children's Oncology Group phase 1 consortium study. Lancet Oncol 2013, 14:472−480
16. Sekimizu M, Osumi T, Fukano R, Koga Y, Kada A, Saito AM, Mori T: A phase I/II study of crizotinib for recurrent or refractory anaplastic lymphoma kinase-positive anaplastic large cell lymphoma and a phase I study of crizotinib for recurrent or refractory neuroblastoma: study protocol for a multicenter single-arm open-label trial. Acta Med Okayama 2018, 72:431−436
17. Alix-Panabieres C, Pantel K: Clinical applications of circulating tumor cells and circulating tumor DNA as liquid biopsy. Cancer Discov 2016, 6:479−491
18. Chicard M, Boyault S, Colmet Daage L, Richer W, Gentien D, Pierron G, Lapouble E, Bellini A, Clement N, Iacono I, Brejon S, Carrere M, Reyes C, Hocking T, Bernard V, Peuchmaur M, Corradini N, Faure-Conter C, Coze C, Plantaz D, Defachelles AS, Thebaud E, Gambart M, Millot F, Valteau-Couanet D, Michon J, Puisieux A, Delattre O, Combaret V, Schleiermacher G: Genomic copy number profiling using circulating free tumor DNA highlights heterogeneity in neuroblastoma. Clin Cancer Res 2016, 22:5564−5573
19. Chicard M, Colmet-Daage L, Clement N, Danzon A, Bohec M, Bernard V, Baulande S, Bellini A, Deveau P, Pierron G, Lapouble E, Janoueix-Lerosey I, Peuchmaur M, Corradini N, Defachelles AS, Valteau- Couanet D, Michon J, Combaret V, Delattre O, Schleiermacher G: Whole-exome sequencing of cell-free DNA reveals temporo-spatial heterogeneity and identifies treatment-resistant clones in neuroblastoma. Clin Cancer Res 2018, 24:939−949
20. Hindson CM, Chevillet JR, Briggs HA, Gallichotte EN, Ruf IK, Hindson BJ, Vessella RL, Tewari M: Absolute quantification by droplet digital PCR versus analog real-time PCR. Nat Methods 2013, 10:1003−1005
21. Hindson BJ, Ness KD, Masquelier DA, Belgrader P, Heredia NJ, Makarewicz AJ, et al: High-throughput droplet digital PCR system for absolute quantitation of DNA copy number. Anal Chem 2011, 83:8604−8610
22. Lodrini M, Sprussel A, Astrahantseff K, Tiburtius D, Konschak R, Lode HN, Fischer M, Keilholz U, Eggert A, Deubzer HE: Using droplet digital PCR to analyze MYCN and ALK copy number in plasma from patients with neuroblastoma. Oncotarget 2017, 8:85234−85251
23. Combaret V, Iacono I, Bellini A, Brejon S, Bernard V, Marabelle A, Coze C, Pierron G, Lapouble E, Schleiermacher G, Blay JY: Detection of tumor ALK status in neuroblastoma patients using peripheral blood. Cancer Med 2015, 4:540−550
24. Combaret V, Turc-Carel C, Thiesse P, Rebillard AC, Frappaz D, Haus O, Philip T, Favrot MC: Sensitive detection of numerical and structural aberrations of chromosome 1 in neuroblastoma by interphase fluorescence in situ hybridization. Comparison with restriction fragment length polymorphism and conventional cytogenetic analyses. Int J Cancer 1995, 61:185−191
25. Castro F, Dirks WG, Fahnrich S, Hotz-Wagenblatt A, Pawlita M, Schmitt M: High-throughput SNP-based authentication of human cell lines. Int J Cancer 2013, 132:308−314
26. Oude Luttikhuis ME, Iyer VK, Dyer S, Ramani P, McConville CM: Detection of MYCN amplification in neuroblastoma using competitive PCR quantitation. Lab Invest 2000, 80:271−273
27. Muth D, Ghazaryan S, Eckerle I, Beckett E, Pohler C, Batzler J, Beisel C, Gogolin S, Fischer M, Henrich KO, Ehemann V,

Gillespie P, Schwab M, Westermann F: Transcriptional repression of SKP2 is impaired in MYCN-amplified neuroblastoma. Cancer Res 2010, 70:3791−3802

28. McDermott U, Iafrate AJ, Gray NS, Shioda T, Classon M, Maheswaran S, Zhou W, Choi HG, Smith SL, Dowell L, Ulkus LE, Kuhlmann G, Greninger P, Christensen JG, Haber DA, Settleman J: Genomic alterations of anaplastic lymphoma kinase may sensitize tumors to anaplastic lymphoma kinase inhibitors. Cancer Res 2008, 68:3389−3395

29. Kumps C, Fieuw A, Mestdagh P, Menten B, Lefever S, Pattyn F, De Brouwer S, Sante T, Schulte JH, Schramm A, Van Roy N, Van Maerken T, Noguera R, Combaret V, Devalck C, Westermann F, Laureys G, Eggert A, Vandesompele J, De Preter K, Speleman F: Focal DNA copy number changes in neuroblastoma target MYCN regulated genes. PLoS One 2013, 8:e52321

30. Amler LC, Schwab M: Amplified N-myc in human neuroblastoma cells is often arranged as clustered tandem repeats of differently recombined DNA. Mol Cell Biol 1989, 9:4903−4913

31. Caren H, Abel F, Kogner P, Martinsson T: High incidence of DNA mutations and gene amplifications of the ALK gene in advanced sporadic neuroblastoma tumours. Biochem J 2008, 416:153−159

32. Hachitanda Y, Saito M, Mori T, Hamazaki M: Application of fluorescence in situ hybridization to detect N-myc (MYCN) gene amplification on paraffin-embedded tissue sections of neuroblastomas. Med Pediatr Oncol 1997, 29:135−138

33. Osajima-Hakomori Y, Miyake I, Ohira M, Nakagawara A, Nakagawa A, Sakai R: Biological role of anaplastic lymphoma kinase in neuroblastoma. Am J Pathol 2005, 167:213−222

34. De Brouwer S, De Preter K, Kumps C, Zabrocki P, Porcu M, Westerhout EM, Lakeman A, Vandesompele J, Hoebeeck J, Van Maerken T, De Paepe A, Laureys G, Schulte JH, Schramm A, Van Den Broecke C, Vermeulen J, Van Roy N, Beiske K, Renard M, Noguera R, Delattre O, Janoueix-Lerosey I, Kogner P, Martinsson T, Nakagawara A, Ohira M, Caron H, Eggert A, Cools J, Versteeg R, Speleman F: Meta-analysis of neuroblastomas reveals a skewed ALK mutation spectrum in tumors with MYCN amplification. Clin Cancer Res 2010, 16:4353−4362

35. Kohl NE, Kanda N, Schreck RR, Bruns G, Latt SA, Gilbert F, Alt FW: Transposition and amplification of oncogene-related sequences in human neuroblastomas. Cell 1983, 35:359−367

36. Duijkers FA, Gaal J, Meijerink JP, Admiraal P, Pieters R, de Krijger RR, van Noesel MM: Anaplastic lymphoma kinase (ALK) inhibitor response in neuroblastoma is highly correlated with ALK mutation status, ALK mRNA and protein levels. Cell Oncol 2011, 34:409−417

37. Corvi R, Amler LC, Savelyeva L, Gehring M, Schwab M: MYCN is retained in single copy at chromosome 2 band p23-24 during amplification in human neuroblastoma cells. Proc Natl Acad Sci U S A 1994, 91:5523−5527

38. Guo C, White PS, Weiss MJ, Hogarty MD, Thompson PM, Stram DO, Gerbing R, Matthay KK, Seeger RC, Brodeur GM, Maris JM: Allelic deletion at 11q23 is common in MYCN single copy neuroblastomas. Oncogene 1999, 18:4948−4957

39. Krishna A, Biryukov M, Trefois C, Antony PM, Hussong R, Lin J, Heinaniemi M, Glusman G, Koglsberger S, Boyd O, van den Berg BH, Linke D, Huang D, Wang K, Hood L, Tholey A, Schneider R, Galas DJ, Balling R, May P: Systems genomics evaluation of the SH-SY5Y neuroblastoma cell line as a model for Parkinson's disease. BMC Genomics 2014, 15:1154

40. Izumi H, Kaneko Y: Evidence of asymmetric cell division and centrosome inheritance in human neuroblastoma cells. Proc Natl Acad Sci U S A 2012, 109:18048−18053

41. Yusuf M, Leung K, Morris KJ, Volpi EV: Comprehensive cytogenomic profile of the in vitro neuronal model SH-SY5Y. Neurogenetics 2013, 14:63−70

42. Kim GJ, Park SY, Kim H, Chun YH, Park SH: Chromosomal aberrations in neuroblastoma cell lines identified by cross species color banding and chromosome painting. Cancer Genet Cytogenet 2001, 129:10−16

43. Corvi R, Savelyeva L, Schwab M: Duplication of N-MYC at its resident site 2p24 may be a mechanism of activation alternative to amplification in human neuroblastoma cells. Cancer Res 1995, 55:3471−3474

44. Thiele CJ: Neuroblastoma Cell Lines. Lancaster, UK: Kluwer Academic Publishers, 1998; 1: 21−53. 1998

45. Van Roy N, Van Limbergen H, Vandesompele J, Van Gele M, Poppe B, Laureys G, De Paepe A, Speleman F: Chromosome 2 short arm translocations revealed by M-FISH analysis of neuroblastoma cell lines. Med Pediatr Oncol 2000, 35:538−540

46. Kryh H, Caren H, Erichsen J, Sjoberg RM, Abrahamsson J, Kogner P, Martinsson T: Comprehensive SNP array study of frequently used neuroblastoma cell lines; copy neutral loss of heterozygosity is common in the cell lines but uncommon in primary tumors. BMC Genomics 2011, 12:443

47. Schmitt M, Pawlita M: High-throughput detection and multiplex identification of cell contaminations. Nucleic Acids Res 2009, 37:e119

48. Gotoh T, Hosoi H, Iehara T, Kuwahara Y, Osone S, Tsuchiya K, Ohira M, Nakagawara A, Kuroda H, Sugimoto T: Prediction of MYCN amplification in neuroblastoma using serum DNA and real-time quantitative polymerase chain reaction. J Clin Oncol 2005, 23:5205−5210

49. Rozen S, Skaletsky H: Primer3 on the WWW for general users and for biologist programmers. Methods Mol Biol 2000, 132:365−386

50. Armbruster DA, Pry T: Limit of blank, limit of detection and limit of quantitation. Clin Biochem Rev 2008, 29 Suppl 1:S49−S52

51. Li H: Aligning sequence reads, clone sequences and assembly contigs with BWA-MEM. arXiv 2013, 1303.3997

52. Faust GG, Hall IM: SAMBLASTER: fast duplicate marking and structural variant read extraction. Bioinformatics 2014, 30:2503−2505

53. Talevich E, Shain AH, Botton T, Bastian BC: CNVkit: genome-wide copy number detection and visualization from targeted DNA sequencing. PLoS Comput Biol 2016, 12:e1004873

54. Kim S, Scheffler K, Halpern AL, Bekritsky MA, Noh E, Kallberg M, Chen X, Kim Y, Beyter D, Krusche P, Saunders CT: Strelka2: fast and accurate calling of germline and somatic variants. Nat Methods 2018, 15:591−594

55. Genomes Project C, Auton A, Brooks LD, Durbin RM, Garrison EP, Kang HM, Korbel JO, Marchini JL, McCarthy S, McVean GA, Abecasis GR: A global reference for human genetic variation. Nature 2015, 526:68−74

56. Fu W, O'Connor TD, Jun G, Kang HM, Abecasis G, Leal SM, Gabriel S, Rieder MJ, Altshuler D, Shendure J, Nickerson DA, Bamshad MJ, Project NES, Akey JM: Analysis of 6,515 exomes reveals the recent origin of most human protein-coding variants. Nature 2013, 493:216−220

57. Ambros PF, Ambros IM, Brodeur GM, Haber M, Khan J, Nakagawara A, Schleiermacher G, Speleman F, Spitz R, London WB, Cohn SL, Pearson AD, Maris JM: International consensus for neuroblastoma molecular diagnostics: report from the International Neuroblastoma Risk Group (INRG) Biology Committee. Br J Cancer 2009, 100:1471−1482

58. Alcaide M, Yu S, Bushell K, Fornika D, Nielsen JS, Nelson BH, Mann KK, Assouline S, Johnson NA, Morin RD: Multiplex droplet digital PCR quantification of recurrent somatic mutations in diffuse large B-cell and follicular lymphoma. Clin Chem 2016, 62:1238−1247

59. Diaz LA Jr, Bardelli A: Liquid biopsies: genotyping circulating tumor DNA. J Clin Oncol 2014, 32:579−586

60. Postel M, Roosen A, Laurent-Puig P, Taly V, Wang-Renault SF: Droplet-based digital PCR and next generation sequencing for monitoring circulating tumor DNA: a cancer diagnostic perspective. Expert Rev Mol Diagn 2018, 18:7−17

61. Combaret V, Audoynaud C, Iacono I, Favrot MC, Schell M, Bergeron C, Puisieux A: Circulating MYCN DNA as a tumor-specific marker in neuroblastoma patients. Cancer Res 2002, 62:3646−3648

62. Combaret V, Hogarty MD, London WB, McGrady P, Iacono I, Brejon S, Swerts K, Noguera R, Gross N, Rousseau R, Puisieux A: Influence of neuroblastoma stage on serum-based detection of MYCN amplification. Ped Blood Cancer 2009, 53:329−331

63. Kojima M, Hiyama E, Fukuba I, Yamaoka E, Ueda Y, Onitake Y, Kurihara S, Sueda T: Detection of MYCN amplification using blood plasma: noninvasive therapy evaluation and prediction of prognosis in neuroblastoma. Pediatr Surg Int 2013, 29:1139−1145

64. Kurihara S, Ueda Y, Onitake Y, Sueda T, Ohta E, Morihara N, Hirano S, Irisuna F, Hiyama E: Circulating free DNA as non-invasive diagnostic biomarker for childhood solid tumors. J Pediatr Surg 2015, 50:2094−2097

65. Iehara T, Yagyu S, Gotoh T, Ouchi K, Yoshida H, Miyachi M, Kikuchi K, Sugimoto T, Hosoi H: A prospective evaluation of liquid biopsy for detecting MYCN amplification in neuroblastoma patients. Jpn J Clin Oncol 2019, 49:743−748

66. Van Roy N, Van Der Linden M, Menten B, Dheedene A, Vandeputte C, Van Dorpe J, Laureys G, Renard M, Sante T, Lammens T, De Wilde B, Speleman F, De Preter K: Shallow whole genome sequencing on circulating cell-free DNA allows reliable noninvasive copy-number profiling in neuroblastoma patients. Clin Cancer Res 2017, 23:6305−6314

67. Vannitamby A, Hendry S, Irving L, Steinfort D, Bozinovski S: Novel multiplex droplet digital PCR assay for scoring PD-L1 in non-small cell lung cancer biopsy specimens. Lung Cancer 2019, 134:233−237

68. Whale AS, Huggett JF, Tzonev S: Fundamentals of multiplexing with digital PCR. Biomol Detect Quantif 2016, 10:15−23

69. Wang HQ, Halilovic E, Li X, Liang J, Cao Y, Rakiec DP, Ruddy DA, Jeay S, Wuerthner JU, Timple N, Kasibhatla S, Li N, Williams JA, Sellers WR, Huang A, Li F: Combined ALK and MDM2 inhibition increases antitumor activity and overcomes resistance in human ALK mutant neuroblastoma cell lines and xenograft models. eLife 2017, 6: e17137